

Trapping and manipulating excited spin states of transition metal compounds

Malcolm A. Halcrow*

Received 11th September 2007

First published as an Advance Article on the web 2nd October 2007

DOI: 10.1039/b701085k

This tutorial review describes how complexes of iron(II) (and, rarely, other metal ions) can be switched between their high- and low-spin states by different physical stimuli. At low temperatures, it is possible to trap a compound in a metastable excited spin-state which, in favourable cases, may be stable to thermal relaxation below temperatures as high as 130 K. The selective switching and trapping of individual spin centres in polynuclear compounds, and the interplay between spin centres as they relax back to their ground states, are also discussed. Similar phenomena, in which spin transitions are coupled to charge transfer phenomena, can also occur in inorganic and metal–organic cyanometallate compounds and in cobalt–semiquinonate complexes.

School of Chemistry, University of Leeds, Woodhouse Lane, Leeds, UK LS2 9JT. E-mail: m.a.halcrow@leeds.ac.uk.

† Magnetic moment data in the literature are quoted as either μ_{eff} or as $\chi_{\text{M}}T$, which are related by

$$\mu_{\text{eff}} = \sqrt{\frac{3k}{N\beta^2} \chi_{\text{M}}T} = 2.828 \sqrt{\chi_{\text{M}}T}$$

Early spin-crossover studies tended to use μ_{eff} , but $\chi_{\text{M}}T$ is often preferred in more recent work because it scales directly with the spin-state population of the sample. A material that is 50% high-spin will show $\chi_{\text{M}}T$ midway between the fully high and fully low-spin values

$$\chi_{\text{M}}T(50\% \text{HS}) = \frac{\chi_{\text{M}}T(\text{HS}) + \chi_{\text{M}}T(\text{LS})}{2}$$

Since μ_{eff} is proportional to the square root of $\chi_{\text{M}}T$, a material that is 50% high-spin will exhibit the less intuitive μ_{eff} value given by

$$\mu_{\text{eff}}(50\% \text{HS}) = \frac{\mu_{\text{eff}}(\text{HS}) + \mu_{\text{eff}}(\text{LS})}{\sqrt{2}}$$



Malcolm A. Halcrow

Malcolm Halcrow obtained his PhD in 1991 at the University of Edinburgh, under Prof. Martin Schröder. He then undertook post-doctoral work in the Laboratoire de Chimie de Coordination du CNRS (Toulouse) with Dr Bruno Chaudret, and at Indiana University with Prof. George Christou. After four years as a Royal Society Research Fellow at the University of Cambridge, in 1998 he moved to the University of Leeds

where he is now Reader. His research interests involve the synthesis and physical characterisation of functional coordination compounds, and metallorganic supramolecular chemistry.

1. Introduction – thermal spin transitions in transition metal complexes

The first spin-crossover compounds were iron(III) dithiocarbamate complexes, whose magnetic moments were shown to be temperature-dependent by Cambi *et al.* in the 1930s (I, Fig. 1).¹ This behaviour was explained as a thermal equilibrium between “magnetic isomers” of the compounds, the high-temperature isomer having $\mu_{\text{eff}} = 5$ BM and the low-temperature isomer $\mu_{\text{eff}} = 1$ BM†. That suggestion was only clarified 30 years later, when the physics behind spin-crossover was first elucidated by Martin *et al.*² The magnetic isomers of

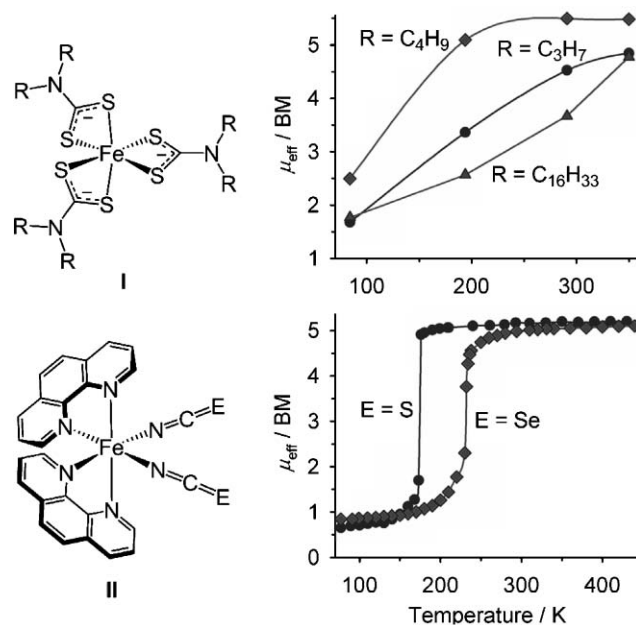
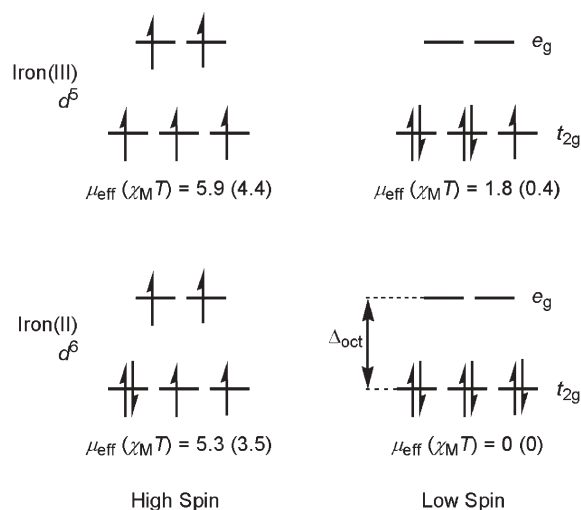


Fig. 1 Selected magnetic data from the first spin-crossover compounds to be discovered containing iron(III) (I)^{1,2} and iron(II) (II),⁶ the metal ions that most commonly show the phenomenon. Data points for each compound are linked by a spline curve for clarity†.

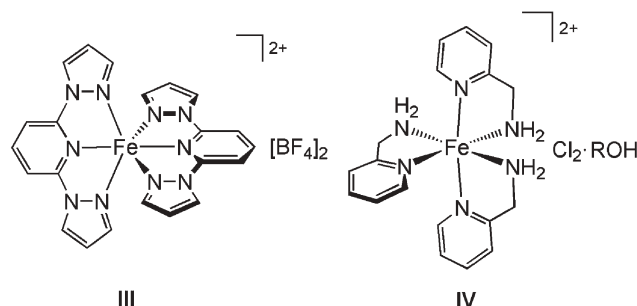


Scheme 1 d-Orbital occupancies and typical values for the magnetic moments of high- and low-spin iron(III) and iron(II) complexes in an octahedral ligand field†. The units of μ_{eff} are Bohr magnetons, and those of $\chi_M T$ are $\text{cm}^3 \text{mol}^{-1} \text{K}$.

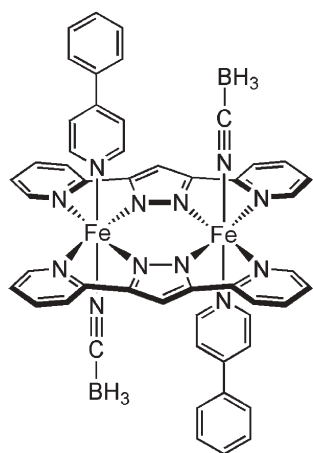
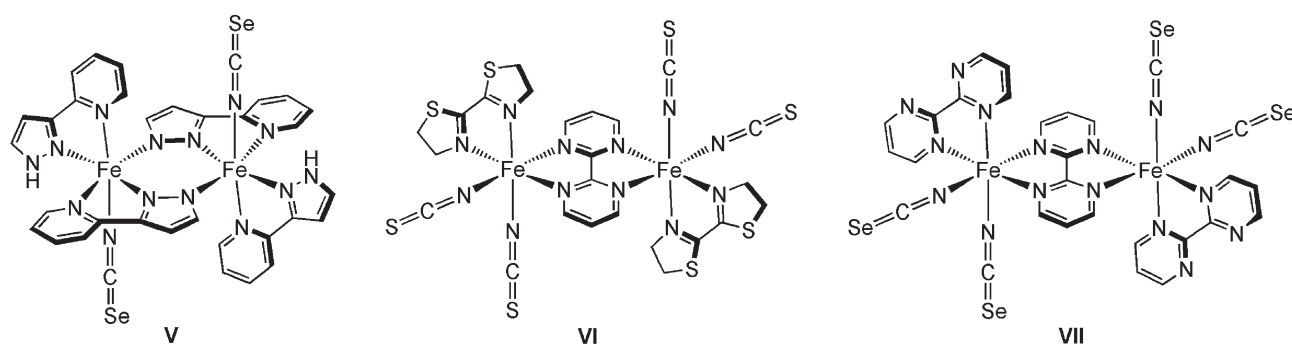
these compounds do not have different chemical structures, as had been proposed. Rather, they reflect the ability of the same molecule to adopt one of two different electronic states, with different distributions of electrons in its frontier d orbitals. The high-spin state contains the maximum possible number of unpaired d-electrons, and is favoured in a ligand field (Δ_{oct} , Scheme 1) that is weaker than the energy required to overcome electrostatic repulsion between pairs of electrons in the same d-orbital (the “pairing energy”). The converse is true for the low-spin state (Scheme 1). In an intermediate ligand field, the energy difference between these two states can be so small that an external stimulus will induce a transition from one to the other. Most commonly this will be a change in temperature, occurring at a point where the higher vibrational and configurational entropy of the high-spin state overcomes the more favourable enthalpy of the stronger M–L bonds in the low-spin form.³ As well as their different magnetic moments, the spin states for a particular metal compound can often be distinguished from their crystallographic M–L bond lengths, which can be up to 10% shorter in the low-spin form; from their UV/vis spectra; or, by other element-specific spectroscopic methods (Mössbauer spectroscopy for iron, EPR for cobalt(II) and iron(III), *etc.*).

Any d^4 – d^7 transition ion may show spin-crossover in principle, but in practise most spin-crossover research is done with six-coordinate iron(II) complexes of N-donor ligands, because these tend to give the most interesting behaviour.^{3,4} However, the phenomenon is also well-established in some classes of octahedral iron(III) (*e.g.* **I**) and cobalt(II) compounds; in certain five-coordinate complexes of iron(II) and iron(III); and, in some inorganic cobalt(III) oxides.⁴ There are also examples of spin-crossover in chromium(II), manganese(II) and manganese(III) chemistry.⁴ While mononuclear compounds of heavier transition elements are low-spin, there are polynuclear niobium and ruthenium compounds that undergo spin-transitions between molecular orbitals involved in metal-metal bonding.⁵

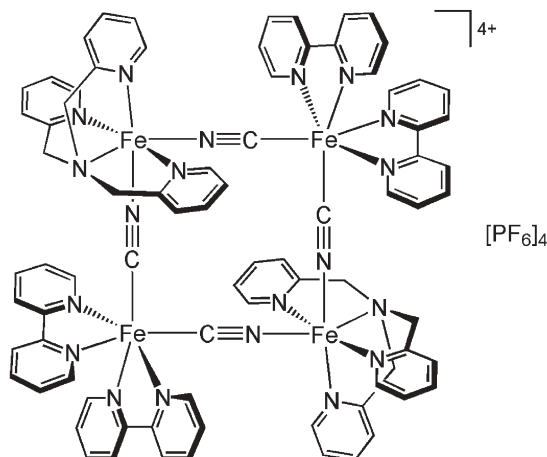
The first iron(II) spin-transition compounds were **II** (Fig. 1) which were recognised as such in 1967, three years after they were first published.⁶ These were also noteworthy as the first known spin-transitions to take place abruptly, rather than over a wide temperature range (Fig. 1). This occurs when the individual spins in the material switch cooperatively, rather than independently of each other. Spin-crossover in solution proceeds gradually with changing temperature, typically occurring over a temperature range spanning 150 K. A much greater variety of thermal spin-transitions is observed in the solid state, ranging from gradual to abrupt transitions that are complete within a temperature range of 1 or 2 K. Thermal hysteresis can also be observed, usually in abrupt transitions, when these are measured in both warming and cooling modes. An abrupt transition reflects cooperativity between the spin centres in the solid, and is therefore a function of the intermolecular packing within the material. The rules for predicting the form of a solid state spin-transition from crystal engineering are still open to question, as illustrated by two contradictory studies. On one hand, a series of six compounds related to **III**, that all form layer structures *via* identical four-fold π – π stacking, exhibit very consistent abrupt thermal spin-crossover with narrow thermal hysteresis.⁷ On the other, six different alcohol solvates of formula **IV** ($R = \text{Me, Et, } n\text{Pr, } i\text{Pr, allyl or } t\text{Bu}$) adopt the same hydrogen-bonded network topology, but all exhibit widely differing spin-transition regimes.⁸ Thus, spin-crossover cooperativity appears to correlate with crystal packing in **III** and its analogues, but not in **IV**. Rationalisation of those observations would be an important step towards the design and production of a spin-transition material from first principles.



Discontinuous or incomplete transitions are also well-known, where fractions of the spin centres in a solid undergo spin-crossover under different conditions from each other. Discontinuities in spin-crossover can reflect crystallographic phase changes, or order/disorder phenomena in the crystal, but are most common in materials containing two or more unique spin sites, which undergo spin-crossover (or not) independently of each other. Particularly important examples of this are dinuclear iron(II) molecules, whose iron atoms may undergo spin-crossover simultaneously (*i.e.* high/high \rightarrow low/low, *e.g.* **V**)⁹ or consecutively (high/high \rightarrow high/low \rightarrow low/low, *e.g.* **VI**)¹⁰ on cooling. Alternatively, the compound may stop half-way (high/high \rightarrow high/low, *e.g.* **VII**).¹¹ To complicate matters, at least one example (**VIII**) is known where the dinuclear molecules in a solid undergo simultaneous



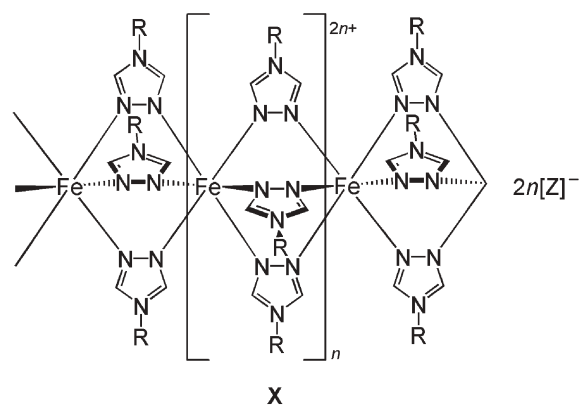
VIII



IX

spin-crossover in two fractions (high/high \rightarrow high/high:low/low \rightarrow low/low).¹² It is difficult to distinguish the types of behaviour shown by compounds VI and VIII without crystallographic data. Larger molecular species that show spin-crossover are rare, and most examples exhibit very gradual and poorly defined transitions. One exception is the molecular square IX, whose two opposite $[\text{Fe}(\text{tpa})]^{2+}$ (tpa = *tris*{pyrid-2-ylmethyl}amine) vertices undergo abrupt spin-crossover at different temperatures on cooling. Crystallographic studies showed that these transitions are site-specific, the first step occurring at one localised $[\text{Fe}(\text{tpa})]^{2+}$ site in the molecule and the second step at the other.¹³ Coordination polymers that undergo spin-crossover are well-known, and show the same types of behaviour as discrete molecular compounds.^{4,14}

Spin-crossover research was further stimulated when Kahn *et al.* discovered in 1993 that some formulations of the chain polymers X (R = alkyl, NH_2 *etc.*; Z^- = a monoanion) undergo a thermal spin-transition, showing a wide hysteresis loop spanning room temperature.¹⁵ In common with many iron(II) complexes, spin-crossover in X is accompanied by a colour change, in this case from colourless (high-spin) to purple (low-spin). The magnetic moment, colour and dielectric constant of this compound are therefore all bistable at room temperature. The use of these materials, and others like them, in displays (using the switch in colour) and digital memory devices (*via* the dielectric switching) have been described and patented.⁴



X

More in-depth discussions of the phenomenology of spin-crossover are available in refs. 3 and 4. The rest of this article is dedicated to an aspect of the field that is developing particularly rapidly; the kinetic trapping of metal centres in excited spin states.

2. Light-induced spin transitions and spin-state trapping

Spin-crossover can be induced photochemically in solution, although like any d-d transition the resultant excited electronic state only has a lifetime around 10^2 ns.⁴ However, Gütllich *et al.* discovered in 1984 that irreversible spin-state conversions can be induced in the solid by laser irradiation.¹⁶ A typical

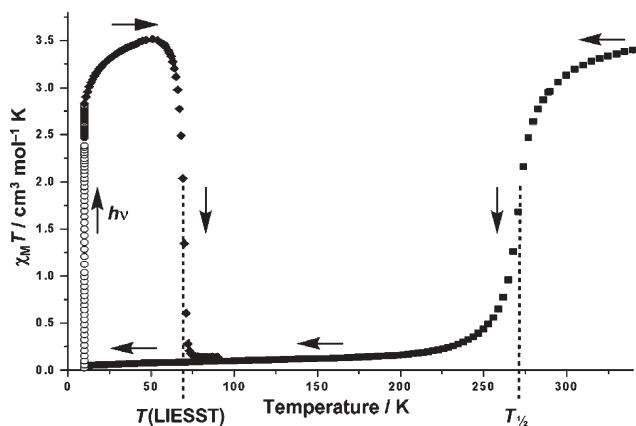


Fig. 2 A LIESST experiment, using a SQUID magnetometer†. Thermal magnetic data (■), sample irradiation at 10 K (○) and LIESST relaxation (◆) of a typical spin-crossover material. See text for more details.

experiment of this type is shown in Fig. 2. The sample in Fig. 2 undergoes a thermal spin-transition upon cooling, with a mid-point temperature $T_{1/2}$ of 271 K. The low-spin material is then irradiated at 10 K, causing $\chi_M T$ to increase as the high-spin state of the material is populated. When a saturation value of $\chi_M T$ is reached, the laser is extinguished and the sample rewarmed. The initial increase in $\chi_M T$ on heating from 10 to 30 K has nothing to do with spin-crossover, but is caused by zero-field splitting of the high-spin state of the compound. The compound remains high-spin upon warming to a temperature where the thermal energy becomes sufficient to overcome the activation barrier to thermal relaxation of the material (in this case, 70 K). $\chi_M T$ then rapidly collapses to its low-spin value of zero. Below 70 K this compound is bistable, and can adopt either its low-spin ground state or a trapped, metastable high-spin excited state, depending on its history. This phenomenon is termed the “Light-Induced Excited Spin-State Trapping” (LIESST) effect, and the relaxation temperature of the trapped excited spin-state is referred to as $T(\text{LIESST})$ (Fig. 2).^{3,4,17}

The metal-to-ligand charge-transfer absorptions of the low-spin form of a compound are usually irradiated with a green laser, converting it to its high-spin form as in Fig. 2. If the temperature is held below their activation barrier for thermal relaxation, the trapped spins can only relax back to their low-spin ground state by quantum-mechanical tunnelling. Tunnelling is inhibited when the ground and excited states of a compound have very different structures, which is particularly the case in iron(II) complexes (Section 3). Some samples can therefore retain their excited spin-state for days at sufficiently low temperatures. Iron(II) materials showing $T(\text{LIESST}) > 50$ K are the exception rather than the rule, but several examples are known where excited spin-states remain trapped at higher temperatures. The current record $T(\text{LIESST})$ for a molecular complex is 132 K (Section 3),¹⁸ but relaxation temperatures up to 145 K have been achieved with some Prussian Blue-type inorganic lattices (Section 5).¹⁹ Complete, 100% conversion during the LIESST process is not always achieved, often because the laser light is absorbed

before it can fully penetrate the solid sample (low-spin metal complexes are usually strongly coloured). For that reason, LIESST experiments are usually performed on just a few mg of powder spread into a thin layer.¹⁷

The “reverse-LIESST” reaction can also be achieved, converting a high-spin species to its low-spin form. This is performed by exciting a metal-based d–d absorption in the high-spin material, using red laser light. However, this d–d band is much less intense than the charge-transfer absorption irradiated in the normal LIESST process. Therefore, the reverse-LIESST photochemical experiment has a much lower quantum yield, and is correspondingly less efficient.

Metastable high-spin forms of spin-transition materials at low temperature can also sometimes be trapped by thermal quenching. That is, by rapid cooling of the sample to a point where the thermal energy is below the activation barrier for the structural rearrangement accompanying spin-crossover. This is most common in systems where spin-crossover occurs below 100 K, so that only a small degree of super-cooling is required. The corollary is that spin-transitions with $T_{1/2} < 100$ K are often incomplete, because a fraction of the sample remains trapped in its high-spin state at normal cooling rates. Spin-state trapping can also be observed following nuclear decay of a ⁵⁷Co nucleus in a high-spin cobalt(II) complex, to a metastable high-spin form of the corresponding ⁵⁷Fe compound (the “Nuclear decay-Induced Excited Spin-State Trapping” or NIESST effect).^{3,4} Metastable high-spin states formed by thermal quenching and by NIESST usually exhibit identical characteristics to their light-generated counterparts, when the comparison has been made.⁴ Exceptions to that generalisation can occur when the LIESST process involves a crystallographic phase change, which is kinetically inhibited during thermal quenching. The two techniques then give the same trapped molecular high-spin state in two different crystal phases, which have differing thermal stabilities (Section 3).

While most LIESST experiments are carried out on powder samples, the technique can also be performed on single crystals. This can afford crystal structures of a compound in two (or more) different electronic states at the same temperature.^{20–26} There are usually small but significant structural differences between high-spin iron(II) complexes in their thermally stable and trapped metastable forms (Fig. 3). This is attributed to different crystal pressures experienced by the molecules at the very different temperatures of the two experiments (typically room temperature and ≤ 30 K), caused by anisotropic contraction of the crystal on cooling. Single crystal LIESST experiments have also been used to demonstrate the presence or absence of a crystallographic phase change during the LIESST reaction (Section 3),²² and to delineate the consequences of these gross structural changes in the solid state. The most complicated example studied so far is $[\text{Fe}(\mu\text{-pmd})(\mu\text{-Ag}\{\text{CN}\}_2)(\mu\text{-Ag}_2\{\text{CN}\}_3)]$ (pmd = pyrimidine), which has a complex self-penetrating 3D network structure containing five crystallographically distinct iron environments.²⁴ This material undergoes thermal spin-crossover in two abrupt steps at $T_{1/2} = 147$ and 185 K, and exhibits the LIESST effect as a powder and single crystals. Relaxation kinetics measurements identified three distinct iron populations with different thermal barriers for LIESST relaxation.

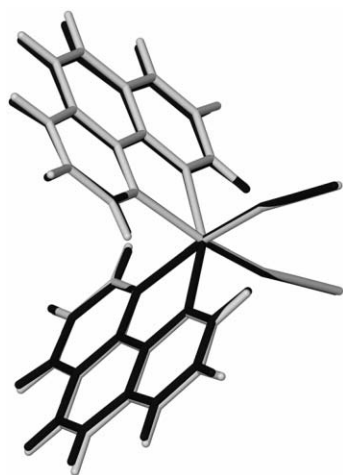


Fig. 3 Overlay of the single crystal structures of the high-spin states of **II** ($E = S$) at 293 K (pale), and generated at 30 K by laser irradiation of the crystal (dark).²¹ The Fe–N bond lengths are up to 0.029(6) Å shorter in the photogenerated structure, and the dihedral angle between the planes of the two 1,10-phenanthroline ligands has contracted by 2.0°.

Crystal structures at different temperatures, and following irradiation at 30 K, showed which of the five iron centres were involved in each step of both processes, and implied that bonding interactions between silver centres in the lattice contribute significantly to the cooperativity of the transition.²⁴

The low temperatures required for the observation of spin-state trapping phenomena might restrict their practical application. However, switching spin states at higher temperatures by irradiation has also been achieved in two different ways. First, is using materials that are genuinely bistable under the conditions of measurement, by performing the experiment at a temperature inside the thermal hysteresis loop of a cooperative spin-transition. Recently the first fully reversible, room temperature light-activated switch of this type was attained using anhydrous $[\text{Fe}(\mu\text{-pyz})(\mu_4\text{-Pt}(\text{CN})_4)]$ (pyz = pyrazine, Fig. 4). This material shows a 24 K spin-crossover hysteresis loop that spans room temperature. It can be shuttled forwards and backwards between its bistable low- and high-spin forms, using individual pulses of the same laser light at room temperature.²⁷ Rather than being a spin-trapping process, this is a genuinely reversible photochromic switch.

The second way of performing light-induced spin-crossover at room temperature, is by irradiating a ligand-based chromophore rather than the metal itself.⁴ Photochemical *cis*–*trans* isomerisation of a styryl group on the periphery of a complex changes the ligand field exerted by the affected ligand. That may in turn cause a partial spin-state change in the sample. This “Ligand-Driven, Light-Induced Spin Crossover” (LD-LISC) can be performed in solution or with samples doped into polymer films, at any temperature where the *cis* and *trans* isomers of the compound have different spin states, including room temperature if appropriate.⁴ It has not been demonstrated in the crystalline state, though, because the large changes in molecular structure required would be inhibited by a rigid solid lattice.

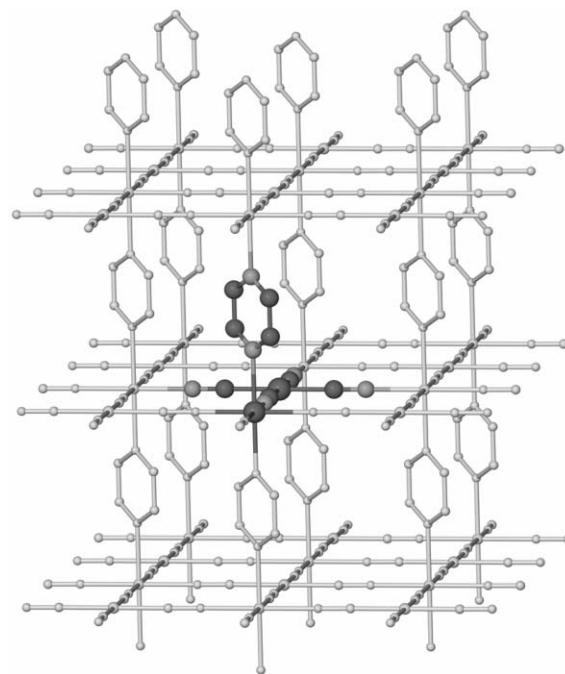
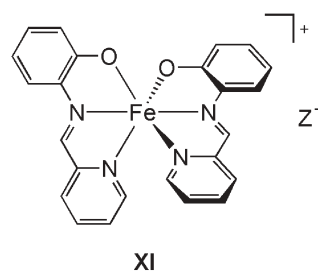


Fig. 4 Fragment of the structure of $[\text{Fe}(\mu\text{-pyz})(\mu_4\text{-Pt}\{\text{CN}\}_4)]$, which undergoes reversible light-induced high/low spin switching at room temperature.²⁷ One formula unit in the lattice is highlighted for clarity.

3. Factors determining the stability of a trapped spin state

Virtually all compounds known to show the LIESST phenomenon are iron(II) complexes with six N-donor ligands. There is a good reason for that; of all the metal ions (Section 1) and ligands that give spin-crossover complexes, the iron(II)/N-ligand combination leads to the greatest change in metal–ligand bond lengths between the high- and low-spin states. So, iron(II) compounds with N-donor ligands give the longest-lived photochemical excited spin-states, since the large structural changes involved inhibit their relaxation by quantum mechanical tunnelling. For example, the rates of tunnelling relaxation of photogenerated high-spin states of spin-crossover iron(II) complexes in low-temperature matrices are up to 10^7 times slower than for comparable iron(III) compounds.⁴ However, solid salts of the iron(III) complex **XI** ($Z^- = \text{ClO}_4^-$ or PF_6^-), and a small number of related iron(III) compounds, do show LIESST spin-trapping with $T(\text{LIESST})$ of up to 105 K.²⁸ Notably, the rigid polyaromatic tridentate ligand used in **XI** follows the qualitative rules established by Létard for the design of long-lived LIESST states, described below.¹⁷ This implies there may be scope to rationally design

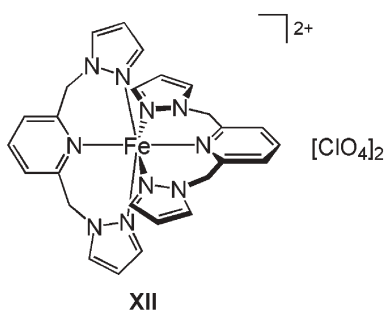


other LIESST systems containing metal ions other than iron(II). The yield of trapped spins in most iron(III) LIESST systems (with one exception) is no more than 25%, however, which may reflect absorption of the exciting laser by the intensely coloured samples.

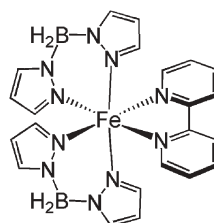
The thermal stability of LIESST excited states is inversely related to their thermal crossover temperature $T_{1/2}$ (the "Inverse Energy Gap Law").⁴ This reflects the fact that the driving force for relaxation is reduced as ΔG between the two spin-states is lowered. However, the stability of a trapped high-spin state also depends significantly on the way it is measured, so only experiments run under the same conditions can be properly compared.¹⁷ Létard's group have built up a library of data run under standardised conditions in their laboratory, and have established that the relationship between the thermodynamic stability of a trapped spin-state, and $T_{1/2}$, can be described by a simple linear relation (eqn 1):

$$T(\text{LIESST}) = T_0 - 0.3T_{1/2} \quad (1)$$

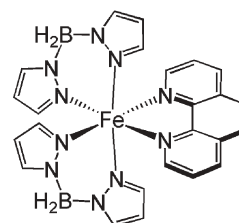
The intercept of this line, T_0 , depends principally on the nature of the ligand sphere surrounding the metal ion.¹⁷ Thus, complexes of monodentate N-donor ligands generally give $T(\text{LIESST})$ values consistent with $T_0 = 100$ K, bidentate ligands afford $T_0 = 120$ K and tridentate ligands $T_0 = 150$ K. This gross correlation also depends on the rigidity of the polydentate ligand itself, however. For example, **III** and **XII** undergo thermal spin-crossover at almost the same $T_{1/2}$, 260 K and 250 K respectively. However while $T(\text{LIESST})$ for **III**, 81 K, is close to that predicted by eqn (1) with $T_0 = 150$ K,²³ $T(\text{LIESST})$ for **XII** is much lower at 38 K.²⁹ That reflects the decreased rigidity of the ligands in **XII**, whose heterocyclic donor groups are separated by a flexible methylene spacer rather than being directly linked.



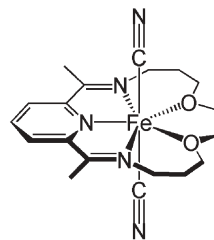
Matters become more complicated when the LIESST process triggers a more profound structural change in the material. For example, **XIII** and **XIV** are isostructural at room temperature, and both undergo abrupt thermal spin transitions near 160 K. However, $T(\text{LIESST})$ for **XIII** (52 K) is significantly higher than for **XIV** (44 K). This is because **XIV** undergoes a crystallographic phase transition during spin-crossover, which is not reversed during LIESST excitation. Conversely, **XIII** retains the same crystal phase in both spin states. Hence, the trapped high-spin states of **XIII** and **XIV** adopt two different crystal phases, which explains their different LIESST relaxation barriers.²²



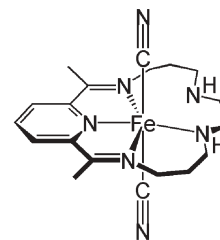
XIII



XIV



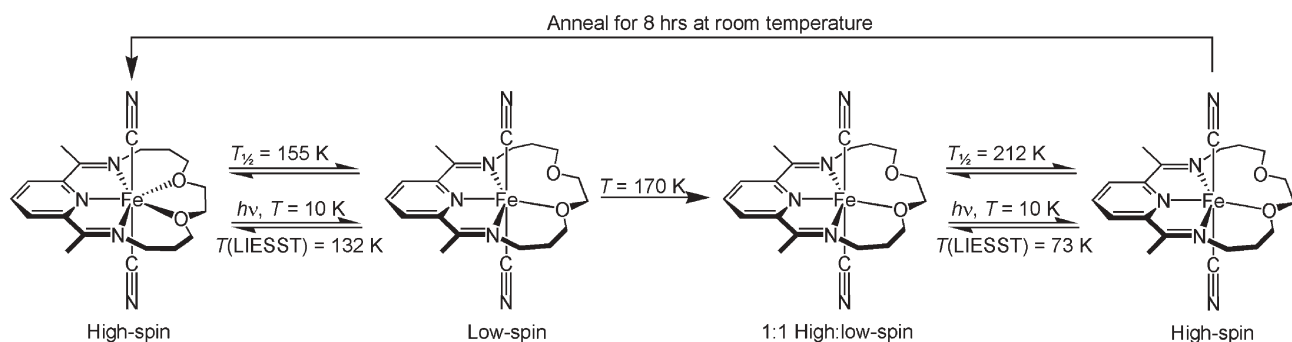
XV



XVI

A more complicated example is the compound that is the current $T(\text{LIESST})$ record holder (**XV**), which has the seven-coordinate structure shown when freshly crystallised. The thermal behaviour of this material is summarised in Scheme 2.¹⁸ An initial cooling step on freshly prepared compound shows a complete, reversible spin-transition with $T_{1/2} = 155$ K. However, upon rewarming to 170 K the low-spin material transforms irreversibly to a different crystal phase, which now has a 1 : 1 high : low-spin population. The mixed-spin phase itself then undergoes reversible spin-crossover to a different high-spin phase at $T_{1/2} = 212$ K. This behaviour is a consequence of a change in coordination geometry during the initial spin transition event, from seven-coordinate high-spin to six-coordinate low-spin (Scheme 2). The resultant low-spin six-coordinate phase is only metastable, and transforms on rewarming to its thermodynamic mixed-spin phase. The six-coordinate high-spin material that is the ultimate product of the thermal cycle is itself metastable at room temperature, but only reverts to the original seven-coordinate high-spin structure after 8 h at 298 K. Both the low-spin and the 1 : 1 mixed-spin phases of **XV** undergo the LIESST excitation to their associated high-spin phases, relaxing at $T(\text{LIESST}) = 132$ and 73 K respectively (Scheme 2).¹⁸ The activation barrier for the ligand rearrangement in the former case leads to a significant increase in the thermal stability of the seven-coordinate LIESST excited state, which contributes to this molecule having the highest known LIESST relaxation temperature.¹⁸ Similar considerations might explain why **XVI** undergoes quantitative LIESST excitation, showing $T(\text{LIESST})$ as high as 105 K, despite being low-spin at room temperature.³⁰ It was proposed that the six-coordinate low-spin compound might transform to a seven-coordinate high-spin species upon irradiation. The additional structural change required to reconvert this to its six-coordinate ground state, would account for the unexpected thermal stability of its trapped high-spin form.

A particularly complicated interplay between thermal spin-crossover and spin-trapping is shown by **XVII**. This undergoes a kinetically slow spin-transition whose temperature depends



Scheme 2 Summary of the spin-transition and phase behaviour of XV under thermal and photochemical cycling.

on the water content of the material, *via* an intermediate mixed-spin phase that the material becomes trapped in if it is cooled too quickly.²⁵ The LIESST effect in compounds related to XVII, like III, obeys eqn (1) with $T_0 = 150$ K.²³ However, eqn (1) would predict $T(\text{LIESST}) \approx 118$ K for fully hydrated XVII ($n = 1/3$); that is above $T_{1/2}$ (105 K), which is impossible. High \rightarrow low spin LIESST relaxation in XVII bypasses the intermediate spin phase from which it was generated, proceeding instead directly to the fully low-spin form (Fig. 5, top). Thus the relaxation follows a different structural pathway

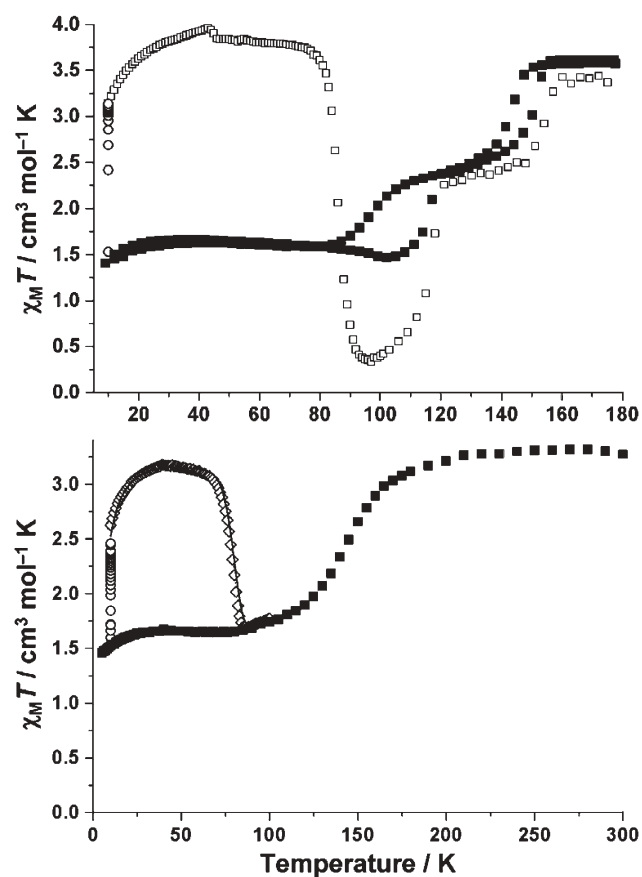
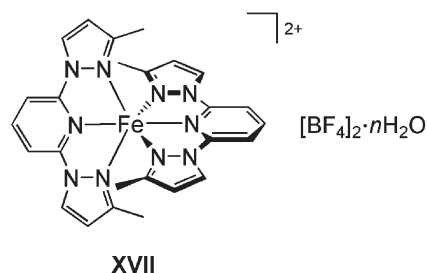


Fig. 5 Top: Thermal magnetic data (■), sample irradiation at 10 K (○) and LIESST relaxation (□) of the mixed-spin phase of XVII.²⁵ Bottom: More typical LIESST behaviour for a mixed-spin phase of a spin-crossover material. The trapped high-spin state relaxes back to the same mixed-spin phase used to generate it.

from thermal spin-crossover, decoupling the two processes and allowing the trapped spin-state to have a lower thermal stability than predicted by eqn (1) (the observed $T(\text{LIESST})$ is 81 K).²⁵ This is the only material known to behave in this way (compare it with the more typical LIESST response from a mixed-spin material shown in Fig. 5, bottom).

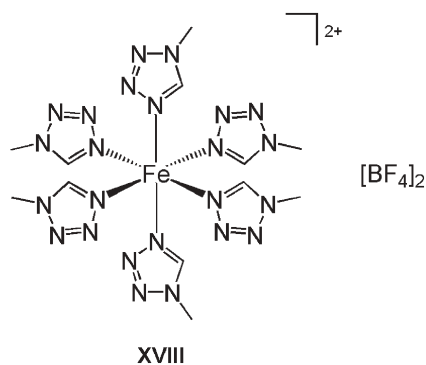


Although eqn (1) implies that the thermodynamic stability of a trapped spin state is only weakly affected by its solid lattice, the kinetics of LIESST relaxation do depend on intermolecular cooperativity. As the reaction proceeds, the increasing crystal pressure experienced by the remaining reactants forces them to relax more quickly. That can lead to significant deviations from Arrhenius behaviour, as the reaction is self-accelerating. If so, the data can be modelled by a stretched exponential method when the deviation from Arrhenius behaviour is small, or by sigmoidal kinetics when the deviation is larger. Both treatments yield an additional energy component, which can be attributed to a cooperativity energy from the surrounding lattice.¹⁷ Cooperative phenomena are not important to spin state relaxation in solution or in frozen matrices. However, the observation of more than one high \rightarrow low spin relaxation rate constant has been used to detect structural equilibria occurring in the metastable high-spin state in solution. These can reflect changes in metal coordination number, or differing conformations in a polydentate ligand backbone.³¹

4. Spin-state trapping in polynuclear systems

Questions of cooperativity in spin-trapping become particularly significant in materials containing more than one iron environment. This can happen in mononuclear compounds with more than one unique molecule in their asymmetric unit, where subtle differences in their molecular structures or local environment mean they have different spin transition regimes.

In that case it can be possible to trap each iron site in either of its spin states individually, by irradiation at different wavelengths and temperatures. For example, crystalline **XVIII** contains two different unique molecular environments in its unit cell. Three different spin states of the compound (high/high, high/low and low/low) have been achieved at the same temperature, by selectively switching either or both of the molecular sites in its powders or single crystals by controlled cooling or irradiation.^{20,32} Modelling the kinetics of relaxation from the trapped high/high-spin and low/low-spin forms of **XVIII**, back to its high/low-spin ground state, afforded the zero-point energy difference between the high- and low-spin states ($\Delta E_{\text{HL}}^0 = \Delta E_{\text{HS}}^0 - E_{\text{LS}}^0$) for the same molecule in two different lattice sites.³²



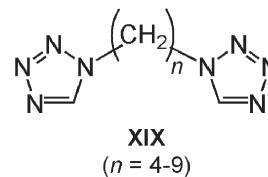
Irradiation of the fully low-spin form of a dinuclear compound usually affords its trapped fully high-spin state, as both metal ions are excited together. However, the two equivalent metal ions in low-spin **VI** have been excited in stepwise fashion, by irradiation at two different wavelengths, leading to distinct metastable high/low (using a near-IR laser) and high/high (using a red laser) forms of the compound.³³ The different results of these photoexcitations may arise because the two wavelengths lead to different initial excited states that give different decay products; or they may reflect the different kinetics of the forward and reverse-LIESST processes (which presumably occur simultaneously) under the two different sets of conditions. Notably, excitation to the high/low spin state in single crystals of **VI** does not eliminate the crystallographic inversion symmetry in the molecule. That is, the first iron atom to be excited is randomly distributed between the two halves of each molecule in the crystal.²⁶

Unusually, the high/low \rightarrow high/high spin photoconversion in **VII** leads to a decrease, rather than an increase, in its magnetic moment at 10 K. This is because the paramagnetic iron centres in its fully high-spin form are antiferromagnetically coupled. That gives the trapped high-spin state a lower net magnetic moment than the isolated paramagnetic iron centre in the mixed-spin ground state, at the low temperature of the experiment.³⁴

The rates of high/high \rightarrow low/low relaxation of the trapped high-spin states of dinuclear compounds are also of interest, in that they give a direct insight into the degree of mechanical cooperativity between metal ions transmitted by bridging ligands. This has been studied in detail for **VI**, whose LIESST relaxation takes place *via* competing one-step

(high/high \rightarrow low/low) and two step (high/high \rightarrow high/low \rightarrow low/low) pathways.¹⁰

LIESST spin-trapping in a small number of 2D and 3D metal-organic coordination polymers has also been reported.^{24,35,36} The thermal stabilities of the trapped high-spin states in such compounds are similar to those shown by mononuclear systems. Also, the kinetics of LIESST relaxation in these materials follow the usual sigmoidal kinetics shown by mononuclear systems with large cooperativity energies. However, one recent study on a series of 3-D iron complex networks $[\text{Fe}(\mu\text{-XIX})_3]\text{Z}_2$ ($\text{Z}^- = \text{BF}_4^-$ or ClO_4^-) has shown that their susceptibility to the LIESST effect depends strongly on the parity of the alkyl chain linking the two tetrazole donors on each ligand.³⁶ Ligands with a C_5 , C_7 or C_9 spacer yield materials showing efficient LIESST trapping, giving metastable materials that relax around 50 K. However, analogous coordination polymers with C_4 , C_6 , C_8 ligand spacers do not exhibit any LIESST effect, showing that relaxation by quantum mechanical tunnelling is much more efficient in the latter compounds. The structural basis underlying this result is unclear, although related “odd-even” effects are also found in other physical properties of compounds with straight-chain alkyl substituents.³⁶ This study emphasises that subtle changes in chemical structure can have a profound influence on the photomagnetism of strongly interacting spin sites, which is still poorly understood.



5. Spin-state transitions and spin trapping by charge transfer

Another type of spin-transition involves charge transfer between redox-active spin sites in a material, and is most developed in heterometallic Prussian Blue analogues, $\text{A}_{2x}\text{M}^{\text{II}}_{1.5-x}[\text{M}^{\text{III}}(\text{CN})_6] \cdot n\text{H}_2\text{O}$ (where A = an alkali metal ion; M^{II} , M^{III} are divalent and trivalent transition ions; and, $0 \leq x \leq 1$).³⁷ These inorganic materials have cubic structures, with octahedral metal centres occupying the vertices of the unit cells and bridging cyano ligands forming the edges of the cubes (Fig. 6). Any alkali metal ions and water molecules present lie in interstitial sites at the centres of the cubes, although water molecules may also coordinate to the divalent metal centres, disrupting a fraction of the cyano bridges in the cubic structure (Fig. 6). Prussian blue itself contains $\text{M}^{\text{II}} = \text{M}^{\text{III}} = \text{iron}$, but related solids with several other divalent or trivalent ions are well known. The stoichiometry of the solids, in the value of x and the degree of hydration, has a strong bearing on their physical properties.

Cobalt/iron materials of type $\text{A}_{2x}\text{Co}_{1.5-x}[\text{Fe}(\text{CN})_6] \cdot n\text{H}_2\text{O}$ can adopt two different combinations of redox and spin. First is low-spin iron(III) ($S = 1/2$) plus high-spin cobalt(II) ($S = 3/2$), leading to a strongly antiferromagnetically coupled material

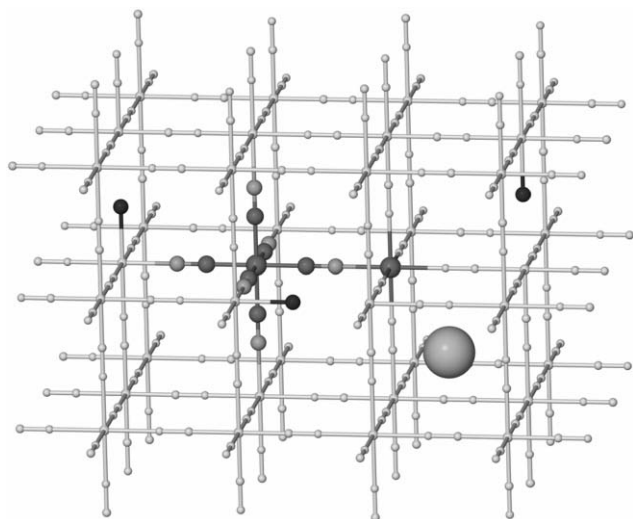


Fig. 6 Fragment of a generic Prussian Blue lattice, $A_{2x}M^{II}_{1.5-x}[M^{III}(CN)_6] \cdot nH_2O$. One $M_2(CN)_6$ formula unit is highlighted for clarity. Disruption of some $\mu-CN^-$ bridges by coordination of water is shown. The centre of one $[M_8(\mu-CN)_{12}]^{8+}$ cube is also highlighted, which will be occupied by other water molecules and/or any A^+ alkali metal ions.

that undergoes bulk ferrimagnetic ordering below a critical temperature (T_c) near 20 K. Second is low-spin iron(II) plus low-spin cobalt(III). These are both diamagnetic ($S = 0$) ions, although materials with this structure usually have a residual paramagnetism from surplus cobalt(II) centres, which decreases as the cobalt : iron stoichiometry approaches unity. These are sometimes termed the “high-temperature” and “low-temperature” phases of the materials, respectively, although examples are known that adopt one or the other form at all temperatures below 300 K.³⁷

Some formulations from the $Na_{2x}Co_{1.5-x}[Fe(CN)_6] \cdot nH_2O$ and $K_{2x}Co_{1.5-x}[Fe(CN)_6] \cdot nH_2O$ families undergo thermal charge-transfer-induced spin transitions (CTIST) between these two states.¹⁹ This usually occurs abruptly with a thermal hysteresis loop around 40 K wide, but the temperature and completeness of the transition depend markedly on the stoichiometry of the material. These CTIST-equilibrium materials also undergo spin trapping upon irradiation with red light^{19,38} or thermal quenching,³⁹ which converts them from paramagnets (low-temperature phase) to ordered ferrimagnets (high-temperature phase) at 5 K. The conceptual similarity between this phenomenon and LIESST is emphasised by the fact that the relaxation temperatures of the trapped CTIST materials follow eqn (1), showing $T_0 = 200$ K.^{17,19} A spin-trapped iron-cobalt prussian blue can also be partially reconverted to its ground state at 5 K, by irradiation with blue light.³⁸ As with spin-crossover compounds (Section 2), an iron-cobalt prussian blue that undergoes thermal CTIST can be shuttled between its two CTIST states by sequential one-shot pulses from the same laser, when poised at a temperature inside the thermal hysteresis loop for the spin equilibrium.⁴⁰

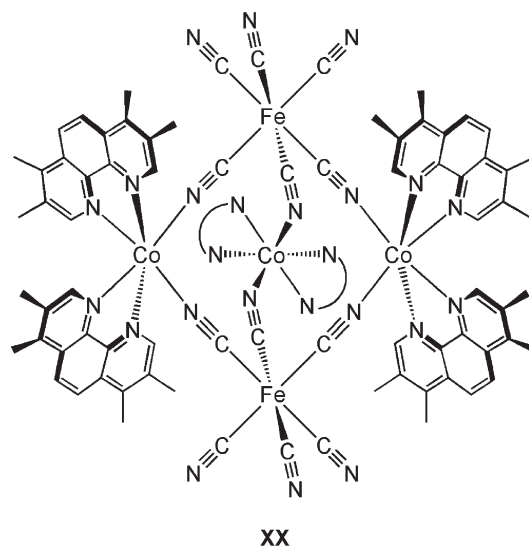
Although the iron-cobalt systems are best studied, thermal and light-induced CTIST phenomena have also been seen

in iron-manganese Prussian Blue analogues and in some conceptually related, mixed-metal molybdenum and tungsten octacyanometallate materials.^{37,41} In contrast, the iron(II) centres in Prussian Blues from the $Cs_{2x}Fe_{1.5-x}[Cr(CN)_6] \cdot nH_2O$ series undergo simple thermal high \rightarrow low spin-crossover at $T_{1/2} \approx 220$ K.⁴² As in the cobalt systems, the net effect of these spin transitions at low temperature is to change the type or degree of the bulk magnetic ordering in the materials, by adding or removing a fraction of paramagnetic spin centres. Spin-trapping in the iron-cobalt, iron-manganese and iron-chromium materials can also be induced by irradiating the samples with synchrotron X-rays, rather than visible light.⁴³

Similar effects have been seen in two molecular species built around polycyanometallate ions. One such compound is **XX**, which can be obtained as three different solid hydrates.⁴⁴ These adopt one of two valence structures, either $[Co^{II}_3Fe^{III}]$ or $[Co^{II}Co^{III}_2Fe^{II}_2]$, distinguishable by their red and blue colouration respectively. One of the red phases undergoes a gradual thermal CTIST upon cooling, as evidenced by a reduction in its magnetic moment and the conversion of 50% of the iron(III) in the material to iron(II) by Mössbauer spectroscopy. On the basis of those data, the low-temperature product of the CTIST equilibrium could be one of two possibilities, which could not be distinguished. Either all the clusters undergo one $Co \rightarrow Fe$ electron transfer event on cooling (eqn 2); or, half the clusters undergo two $Co \rightarrow Fe$ electron transfers (eqn 3).



The products of eqn (2) and eqn (3) both have equal numbers of iron(II) and iron(III) centres, as observed.⁴⁴

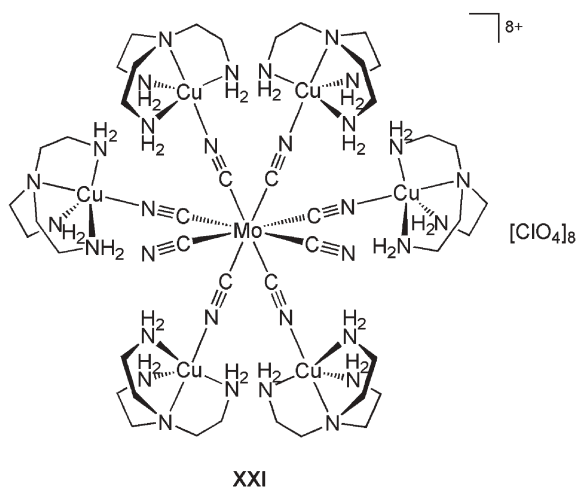


The other example is **XXI**, containing $[Cu(tren)]^{2+}$ centres (tren = tris{2-aminoethyl}amine) appended to six of the eight cyano groups of a $[Mo(CN)_8]^{4-}$ ion.⁴⁵ These compounds do not undergo a thermal CTIST equilibrium on cooling. However, irradiation of **XXI** at 10 K with a blue

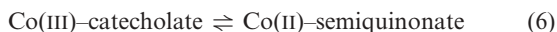
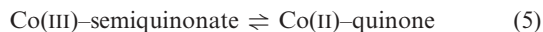
laser causes an irreversible Mo → Cu electron transfer to take place (eqn 4):



The copper centres in the starting material are weakly antiferromagnetically coupled through the diamagnetic molybdenum(IV) centres. In the product, the paramagnetic molybdenum(V) ion is strongly ferromagnetically coupled to the remaining copper(II) centres. So, irradiation causes a sharp increase in magnetic moment of the material at low temperatures. Interestingly, the trapped ferromagnetic state of the compound relaxes very gradually on rewarming to room temperature, contrasting with the rapid decay seen for LIESST excited states when the thermal relaxation temperature is reached. None-the-less, after annealing the irradiated material at room temperature for 1 h the $\text{Mo}^{\text{IV}}\text{Cu}^{\text{II}}_6$ ground state was fully restored.⁴⁵ Spin-trapping has also been reported in the inorganic lattice $\text{CuMo}(\text{CN})_8$.⁴¹ Although its effect on the magnetic behaviour of that material is rather different, the underlying origin of the effects observed is the same as in **XXI**. The molecular complex can be thought of as a model for the inorganic material in this case.

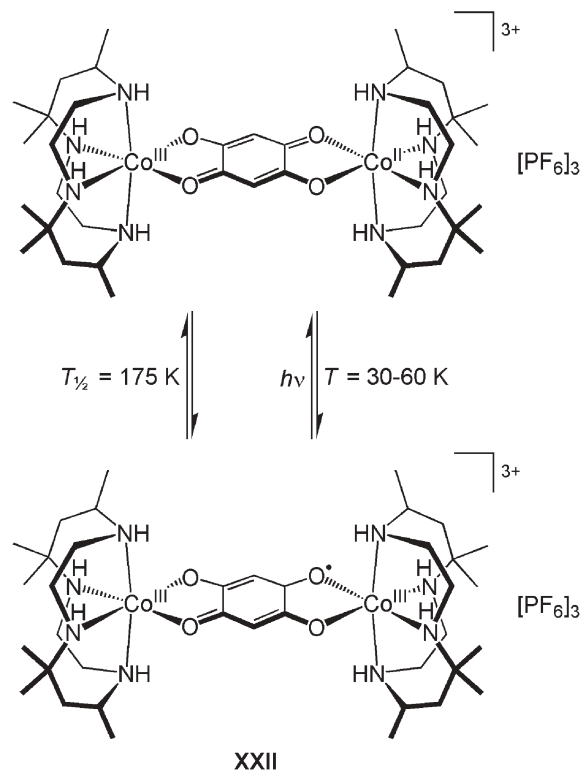


Related photomagnetic phenomena have also been seen in some cobalt/*ortho*-semiquinonato complexes.⁴⁶ Such compounds can undergo either of the following, reversible valence-tautomeric processes on cooling (eqn 5 and 6), depending on their oxidation level:⁴



This is effectively a metal-organic CTIST phenomenon, although it has not been called that in the literature. These processes usually involve a concomitant low → high-spin transition at the cobalt ion, and so lead to a strong change in magnetic moment. They are also easily monitored by following the appearance or disappearance of the semiquinonate ligand radical signal by EPR.

One example from several⁴⁶ is the dinuclear compound **XXII** (Scheme 3). $\chi_{\text{M}}T$ for this complex decreases gradually from



Scheme 3 Thermally and light-activated valence tautomerism in a mixed-valence, dinuclear cobalt dioxolene complex.⁴⁷

$2.5 \text{ cm}^3 \text{ mol}^{-1} \text{ K}$ at 200 K (characteristic of one high-spin cobalt(II) centre) to $0.45 \text{ cm}^3 \text{ mol}^{-1} \text{ K}$ at 10 K (corresponding to a species with one unpaired electron).⁴⁷ EPR spectroscopy confirmed that the low-temperature form has the formulation Co^{III}_2 -semiquinonate, with a ligand radical spin, leading to assignment of the valence tautomerism equilibrium shown in the Scheme. Irradiation of the material at 10 K with green laser light induces the reverse transformation, leading to a trapped mixed-valent material that is stable below 30 K, but has fully relaxed on rewarming to 60 K. Although the yield of spin-trapped centres in bulk material was only 43%, reflectivity measurements showed that quantitative photo-conversion took place at the surface of the sample. Hence, the less efficient spin trapping in powder samples of **XXII** is simply a consequence of poor light penetration into the dark purple material.⁴⁷

6. Conclusions

Several classes of compounds, that undergo different types of thermal spin equilibria, have been shown to exhibit spin trapping at low temperatures. The success of the experiment requires high energy barriers for relaxation of the excited spin state, thermally and by quantum mechanical tunnelling. Both these mechanisms are disfavoured when the relaxation process involves a large structural rearrangement. That criterion is met particularly well by iron(II) complexes which, of the metal ions known to show spin-crossover, give rise to the largest structural differences between their high-spin and low-spin forms. This is why most of the examples cited in this article

involve iron(II), either as a spin-crossover centre or as a component in a CTIST equilibrium. The structural changes required for spin-state relaxation are also disfavoured in a rigid local environment. Hence, although thermal spin-crossover has been measured in several different phases of matter, spin-trapping is purely a solid state phenomenon. The rigidity of the ligand sphere about the metal centre has a greater influence than the nature of the solid lattice, on the thermal stability of a trapped spin state.¹⁷ The best illustration of these criteria is **XV**, where a change in coordination number between spin states and a conformationally restricted macrocyclic ligand combine to produce the highest known *T*(LIESST) for a molecular compound.¹⁸ Extending *T*(LIESST) above 132 K is highly desirable for device applications, and is likely to require an iron(II) material showing a similar combination of structural properties.

Thermal spin-crossover materials have been incorporated into several prototype switchable devices,⁴ but no similar application of spin-trapping has yet been demonstrated. Addressing individual domains of a spin-transition material, at a temperature below *T*(LIESST) or inside a spin-crossover hysteresis loop, using micrometre-wide laser pulses would be an attractive goal. Polycrystalline thin films of spin-transition compounds of the type required for such an experiment, 20–30 nm thick, have recently been prepared.⁴⁸ Importantly, these show thermal spin-crossover responses that are only mildly inferior to those of the bulk solids. The thinnest layer that the LIESST effect has been detected in, so far, is a Langmuir Blodgett film around 1 μm thick.⁴⁹ Spin-trapping in these new nanometre thin films might also be achievable, and would be an important step towards nanotechnological application.

Acknowledgements

Our own research in this area has been funded by the EPSRC, and the British Council/CNRS Alliance bilateral action. The photomagnetic data in Fig. 2 and 5, and the graphical abstract, were run by Dr C. Carbonera or T. Forestier in Dr J.-F. Létard's laboratory (ICMCB, CNRS, Bordeaux), using samples prepared in Leeds by Dr J. Elhaïk or MAH.

References

- 1 L. Cambi and L. Szegő, *Ber. Dtsch. Chem. Ges.*, 1933, **66**, 656 and refs. therein.
- 2 A. H. Ewald, R. L. Martin, I. G. Ross and A. H. White, *Proc. R. Soc. London, Ser. A*, 1964, **280**, 235.
- 3 P. Gülich, Y. Garcia and H. A. Goodwin, *Chem. Soc. Rev.*, 2000, **29**, 419 and ref. therein.
- 4 *Spin Crossover in Transition Metal Compounds I–III*, *Top. Curr. Chem.*, ed. P. Gülich and H. A. Goodwin, 2004, **233–235**, and individual chapters therein.
- 5 H. Imoto and A. Simon, *Inorg. Chem.*, 1982, **21**, 308; P. Angaridis, F. A. Cotton, C. A. Murillo, D. Villagrán and X. Wang, *J. Am. Chem. Soc.*, 2005, **127**, 5008.
- 6 E. König and K. Madeja, *Inorg. Chem.*, 1967, **6**, 48.
- 7 R. Pritchard, C. A. Kilner and M. A. Halcrow, *Chem. Commun.*, 2007, 577 and ref. therein.
- 8 M. Hostettler, K. W. Törnroos, D. Chernyshov, B. Vangdal and H.-B. Bürgi, *Angew. Chem., Int. Ed.*, 2004, **43**, 4589.
- 9 B. A. Leita, B. Moubaraki, K. S. Murray, J. P. Smith and J. D. Cashion, *Chem. Commun.*, 2004, 156.

- 10 A. B. Gaspar, V. Ksenofontov, S. Reiman, P. Gülich, A. L. Thompson, A. E. Goeta, M. C. Muñoz and J. A. Real, *Chem.–Eur. J.*, 2006, **12**, 9289.
- 11 J. A. Real, I. Castro, A. Bousseksou, M. Verdaguer, R. Burriel, J. Linares and F. Varret, *Inorg. Chem.*, 1997, **36**, 455.
- 12 K. Nakano, S. Kawata, K. Yoneda, A. Fuyuhiko, T. Yagi, S. Nasu, S. Morimoto and S. Kaizaki, *Chem. Commun.*, 2004, 2892.
- 13 M. Nihei, M. Ui, M. Yokota, L. Han, A. Maeda, H. Kishida, H. Okamoto and H. Oshio, *Angew. Chem., Int. Ed.*, 2005, **44**, 6484.
- 14 C. J. Kepert, *Chem. Commun.*, 2006, 695.
- 15 J. Kröber, E. Codjovi, O. Kahn, F. Grolière and C. Jay, *J. Am. Chem. Soc.*, 1993, **115**, 9810.
- 16 S. Decurtins, P. Gülich, C. P. Köhler, H. Spiering and A. Hauser, *Chem. Phys. Lett.*, 1984, **105**, 1.
- 17 J.-F. Létard, *J. Mater. Chem.*, 2006, **16**, 2550 and refs. therein.
- 18 S. Hayami, Z.-Z. Gu, Y. Einaga, Y. Kobayashi, Y. Ishikawa, Y. Yamada, A. Fujishima and O. Sato, *Inorg. Chem.*, 2001, **40**, 3240; P. Guionneau, F. Le Gac, A. Kaiba, J. S. Costa, D. Chasseau and J.-F. Létard, *Chem. Commun.*, 2007, 3723.
- 19 N. Shimamoto, S.-I. Ohkoshi, O. Sato and K. Hashimoto, *Inorg. Chem.*, 2002, **41**, 678.
- 20 J. Kusz, H. Spiering and P. Gülich, *J. Appl. Crystallogr.*, 2001, **34**, 229.
- 21 M. Marchivie, P. Guionneau, J. A. K. Howard, G. Chastanet, J.-F. Létard, A. E. Goeta and D. Chasseau, *J. Am. Chem. Soc.*, 2002, **124**, 194.
- 22 A. L. Thompson, A. E. Goeta, J. A. Real, A. Galet and M. C. Muñoz, *Chem. Commun.*, 2004, 1390.
- 23 V. A. Money, I. R. Evans, M. A. Halcrow, A. E. Goeta and J. A. K. Howard, *Chem. Commun.*, 2003, 158; C. Carbonera, J. S. Costa, V. A. Money, J. Elhaïk, J. A. K. Howard, M. A. Halcrow and J.-F. Létard, *Dalton Trans.*, 2006, 3058.
- 24 V. Niel, A. L. Thompson, A. E. Goeta, C. Enachescu, A. Hauser, A. Galet, M. C. Muñoz and J. A. Real, *Chem.–Eur. J.*, 2005, **11**, 2047.
- 25 V. A. Money, C. Carbonera, J. Elhaïk, M. A. Halcrow, J. A. K. Howard and J.-F. Létard, *Chem.–Eur. J.*, 2007, **13**, 5503.
- 26 E. Trzop, M. Buron-Le Cointe, H. Cailleau, L. Toupet, G. Molnár, A. Bousseksou, A. B. Gaspar, J. A. Real and E. Collet, *J. Appl. Crystallogr.*, 2007, **40**, 158.
- 27 S. Bonhommeau, G. Molnár, A. Galet, A. Zwick, J. A. Real, J. J. McGarvey and A. Bousseksou, *Angew. Chem., Int. Ed.*, 2005, **44**, 4069.
- 28 See e.g. S. Hayami, Z.-Z. Gu, M. Shiro, Y. Einaga, A. Fujishima and O. Sato, *J. Am. Chem. Soc.*, 2000, **122**, 7126; K. Takahashi, H. B. Cui, H. Kobayashi, Y. Einaga and O. Sato, *Chem. Lett.*, 2005, **34**, 1240.
- 29 C. Enachescu, J. Linares, F. Varret, K. Boukhedaden, E. Codjovi, S. G. Salunke and R. Mukherjee, *Inorg. Chem.*, 2004, **43**, 4880.
- 30 J. S. Costa, C. Balde, C. Carbonera, D. Denux, A. Wattiaux, C. Desplanches, J.-P. Ader, P. Gülich and J.-F. Létard, *Inorg. Chem.*, 2007, **46**, 4114.
- 31 See e.g. C. Brady, P. L. Callaghan, Z. Ciunik, C. G. Coates, A. Dössing, A. Hazell, J. J. McGarvey, S. Schenker, H. Toftlund, A. X. Trautwein, H. Winkler and J. A. Wolny, *Inorg. Chem.*, 2004, **43**, 4289.
- 32 R. Hinek, P. Gülich and A. Hauser, *Inorg. Chem.*, 1994, **33**, 567.
- 33 N. Ould-Moussa, E. Trzop, S. Mouri, S. Zein, G. Molnár, A. B. Gaspar, E. Collet, M. Buron-Le Cointe, J. A. Real, S. Borshch, K. Tanaka, H. Cailleau and A. Bousseksou, *Phys. Rev. B: Condens. Matter Mater. Phys.*, 2007, **75**, 054101.
- 34 G. Chastanet, J.-F. Létard, A. B. Gaspar and J. A. Real, *Chem. Commun.*, 2001, 819.
- 35 See e.g. V. Niel, M. C. Muñoz, A. B. Gaspar, A. Galet, G. Levchenko and J. A. Real, *Chem.–Eur. J.*, 2002, **8**, 2446; V. Niel, A. Galet, A. B. Gaspar, M. C. Muñoz and J. A. Real, *Chem. Commun.*, 2003, 1248.
- 36 A. Absmeier, M. Bartel, C. Carbonera, G. N. L. Jameson, P. Weinberger, A. Caneschi, K. Mereiter, J.-F. Létard and W. Linert, *Chem.–Eur. J.*, 2006, **12**, 2235.
- 37 A. Dei, *Angew. Chem., Int. Ed.*, 2005, **44**, 1160 and refs. therein.
- 38 O. Sato, T. Iyoda, A. Fujishima and K. Hashimoto, *Science*, 1996, **272**, 704.

- 39 S. Gawali-Salunke, F. Varret, I. Maurin, C. Enachescu, M. Malarova, K. Boukheddaden, E. Codjovi, H. Tokoro, S. Ohkoshi and K. Hashimoto, *J. Phys. Chem. B*, 2005, **109**, 8251.
- 40 H. W. Liu, K. Matsuda, Z. Z. Gu, K. Takahashi, A. L. Cui, R. Nakajima, A. Fujishima and O. Sato, *Phys. Rev. Lett.*, 2003, **90**, 167403.
- 41 S.-I. Ohkoshi, H. Tokoro, T. Hozumi, Y. Zhang, K. Hashimoto, C. Mathonière, I. Bord, G. Rombaut, M. Verelst, C. C. Moulin and F. Villain, *J. Am. Chem. Soc.*, 2006, **128**, 270.
- 42 W. Kosaka, K. Nomura, K. Hashimoto and S. Ohkoshi, *J. Am. Chem. Soc.*, 2005, **127**, 8590.
- 43 S. Margadonna, K. Prassides and A. N. Fitch, *Angew. Chem., Int. Ed.*, 2004, **43**, 6316; D. Papanikolaou, S. Margadonna, W. Kosaka, S. Ohkoshi, M. Brunelli and K. Prassides, *J. Am. Chem. Soc.*, 2006, **128**, 8358.
- 44 C. P. Berlinguette, A. Dragulescu-Andrasi, A. Sieber, H.-U. Güdel, C. Achim and K. R. Dunbar, *J. Am. Chem. Soc.*, 2005, **127**, 6766.
- 45 J. M. Herrera, V. Marvaud, M. Verdaguer, J. Marrot, M. Kalisz and C. Mathonière, *Angew. Chem., Int. Ed.*, 2004, **43**, 5468.
- 46 O. Sato, A. Cui, R. Matsuda, J. Tao and S. Hayami, *Acc. Chem. Res.*, 2007, **40**, 361.
- 47 C. Carbonera, A. Dei, J.-F. Létard, C. Sangregorio and L. Sorace, *Angew. Chem., Int. Ed.*, 2004, **43**, 3136.
- 48 S. Cobo, G. Molnár, J. A. Real and A. Bousseksou, *Angew. Chem., Int. Ed.*, 2006, **45**, 5786; M. Matsuda and H. Tajima, *Chem. Lett.*, 2007, 700.
- 49 J.-F. Létard, O. Nguyen, H. Soyer, C. Mingotaud, P. Delhaes and O. Kahn, *Inorg. Chem.*, 1999, **38**, 3020.

Find a SOLUTION

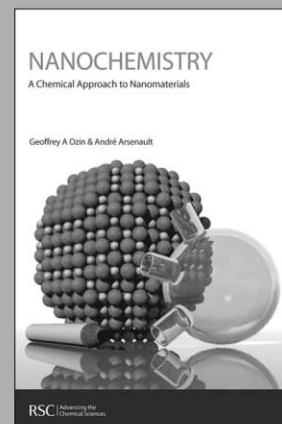
... with books from the RSC

Choose from exciting textbooks, research level books or reference books in a wide range of subject areas, including:

- Biological science
- Food and nutrition
- Materials and nanoscience
- Analytical and environmental sciences
- Organic, inorganic and physical chemistry

Look out for 3 new series coming soon ...

- RSC Nanoscience & Nanotechnology Series
- Issues in Toxicology
- RSC Biomolecular Sciences Series



RSC Publishing

www.rsc.org/books